

Green synthesis and characterization of Ni/NiO magnetic nanoparticles in water

Faezeh Farzaneh* and Sara Haghshenas Kashanie

Department of Chemistry, University of Alzahra, Vanak, Tehran, Iran

Ni/NiO magnetic nanoparticles was prepared using $\text{Ni}(\text{CH}_3\text{COO})_2 \cdot 4\text{H}_2\text{O}$ as starting material, acetylacetonate (AcAc) as template and water as a green solvent under reflux condition, followed by the calcination at 400 °C. The product was characterized by X-ray diffraction (XRD), scanning electron microscopy (SEM), transmission electron microscopy (TEM), and Fourier transform infrared (FT-IR). The size distribution of individual particles were determined to be about 18-20 nm. The prepared magnetic nanoparticles was found to be a good adsorbent for Congo red from solution.

Key words: Ni/NiO, Magnetic nanoparticles, Template, Adsorption.

Introduction

Nanocrystalline magnetic materials have extensively been investigated due to their interesting deviations in magnetic, optical, electrical and thermal properties in comparison to those of their bulk counterparts [1, 2]. Fabrication of metal-metal oxide core-shell nanoparticles (NPs) is an important research area, as it represents different and fascinating possibilities like shell-driven magnetization stability [3-5] and improving contrast to enhance magnetic resonance imaging [6]. In fact, magnetic nanoparticles (MNPs) and nanoassemblies with uniform size distribution are currently of emerging interest because of their extensive applications in memory storage devices, catalysis, sensors, MRI, magnetically controlled drug delivery and hyperthermia treatment of tumor cells [6-8]. Magnetic particles are also one of the most popular materials with increasingly use in immobilizing proteins, enzymes, and other bioactive agents in analytical biochemistry, medicine, and biotechnology [8-10]. Numerous synthetic methods have been developed for the synthesis of MNPs [11] including co-precipitation, [12] sol-gel, [13] microemulsion, [14] and processes such as sonochemical reaction, [15] hydrothermal reaction, [16] thermal decomposition, [17] electrospray synthesis [18] and laser pyrolysis [19].

In nanometer-sized Ni/NiO, the overall magnetic behavior comprising the magnetic nanocrystals of Ni and NiO is the result of the properties of the individual constituents as an intrinsic parameters like the size, shape, and structure. However, assemblies of nanocrystals, containing an interface between a

ferromagnet (FM; Ni) and an antiferromagnet (AFM; NiO) exhibit an additional unidirectional anisotropy owing to magnetic coupling at the FM/AFM interface (exchange bias), which leads to magnetization stability [20, 21]. In nanometer-scale systems, the key factor in magnetic interaction is controlling the volume, shape, crystallinity, and structure of both the FM and AFM materials [22-24].

Nevertheless, as a ceramic material, the mechanical properties of nickel oxide are poor in comparison to those of some oxide ceramics such as silica, alumina or zirconia. In contrast to the metallic nickel, the nickel oxide presents higher hardness and lower fracture toughness [25-27]. Therefore, Ni/NiO either in composites or structures with optimized mechanical properties are pursued [28, 29].

The adsorption of various dyes from aqueous solutions has proven to be an excellent and effective technique in effluent treatment. Several studies have shown that numerous low cost materials have been successfully applied in the removal of dyes from aqueous solutions [30-32]. On the basis of the above-mentioned properties of MNPs, herein we report the facile preparation method for Ni/NiO MNPs in water as a green solvent and AcAc as template and its utilization as adsorption capacity for magnetically separation of Congo Red (CR).

Experimental Details

All chemical materials were purchased from Merck Chemical Company and used without further purification. In a typical synthesis, NaOH pellets (1mmol) and $\text{Ni}(\text{CH}_3\text{COO})_2 \cdot 4\text{H}_2\text{O}$ (1 mmol) were dissolved in deionized water (25 mL) to give a homogenous solution. Acetylacetone (0.49 mL) was subsequently added and the mixture was kept magnetic stirring for 0.5 h followed by heating at reflux over

*Corresponding author:
Tel : +9821 8825897
Fax: +982166495291
E-mail: farzaneh@alzahra.ac.ir

6 hrs. The solid was then filtered, washed with deionized water to remove the impurities, and dried at room temperature. Finally, the product was calcined at 400 °C within 3-5 hrs. The Ni content was determined to be 60.55%.

The product was characterized by X-ray diffraction using a PW1800 diffractometer with Cu k_{α} radiation ($k_{\alpha} = 0.15405$ nm), scanning electron microscopy (SEM, S-4160 Hitachi) and transmission electron microscopy (TEM, Philips EM 208s) at an accelerating voltage of 100 kV. Dye concentration was estimated by monitoring dye absorption intensity at the maximum absorption wavelength using a UV/Vis (Perkin Elmer, Lambda 35). Fourier transformation infrared (FT-IR) spectra were recorded on TENSOR27 spectrophotometer using KBr pellets. Thermal studies were performed, in air using STA 1500 at a heating rate of 10 °C/min. The magnetic properties of samples were measured by Meghnatis Daghigh Kavir Co., vibrating sample magnetometer (VSM) at room temperature. The maximum applied field was 9000 Oe. Atomic absorption spectrometric measurements were carried out using a GVC atomic absorption spectrometer.

Catalytic activity determination

Catalytic activity of the prepared nano Ni/NiO was evaluated by the adsorption of Congo red. 0.05 g of the nano powder was poured into 100 mL aqueous solution of dye (5 ppm) in a glass reaction cell. The set up experiment was kept in the dark and the solution was continuously stirred with a magnetic stirrer. During the reaction, the adsorbed dye was sampled in regular intervals and the dye concentration was monitored by measuring the absorbance of the solution with UV-Vis spectrophotometer.

Results and Discussion

The X-ray diffraction (XRD) pattern of the prepared nanomagnet, with acetylacetonate is shown in Fig. 1. Whereas the three peaks appearing at 37.15°, 43.32° and 62.89° with (003), (012) and (110) reflections is consistent with rhombohedral phase of NiO (JCPDS card no. 22-1189), the other peaks displaying at 44.36, 51.71 and 76.22 with reflection planes (111), (200) and (220) correspond to FCC metallic nickel (JCPDS card no.4-0850) as a second phase. Therefore, the presence of metallic nickel and nickel oxide in the prepared nanomagnet is confirmed.

The SEM, EDX, TEM and SAED of calcined Ni/NiO at 400 °C are given in Fig. 2(a-d), respectively. Based on the SEM (Fig. 2(a)) and EDX (Fig. 2(b)) results, formation of nanoparticles with the average size of 20 nm and presence of Ni with no impurity is evident. The transmission electron microscopy (TEM) also reveals the photographs of Ni/NiO (Fig. 2(c)). The size of nanoparticles obtained from the XRD

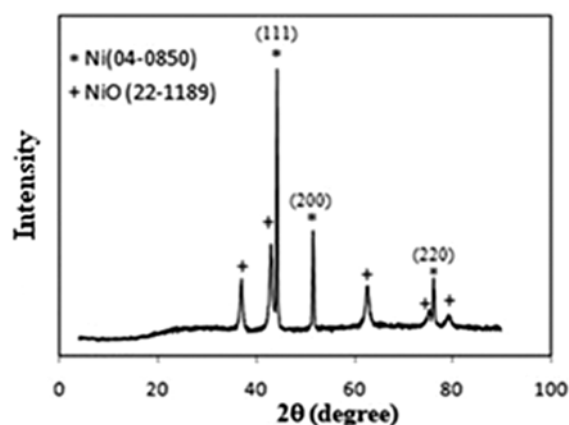


Fig. 1. XRD patterns of Ni/ NiO sample prepared under reflux condition.

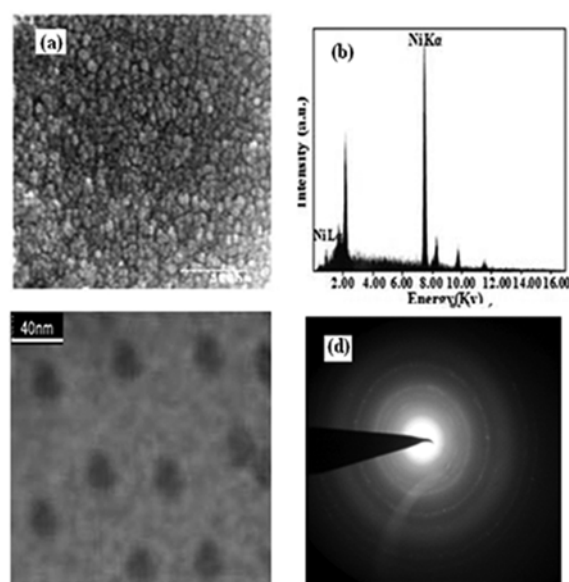


Fig. 2. (a) The SEM image, (b) EDX, (c) TEM, (d) SAED of Ni/NiO MNPs.

diffraction patterns are in close agreement with the TEM studies which exhibit particle sizes of about 18-20 nm. The good crystallinity of the prepared nanoparticles is evident on the basis of the selected area diffraction (SAED) pattern as indicated in Fig. 2(d).

The FT-IR spectra of nickel acetate tetrahydrate, acetyl acetone, the as prepared and calcined nanomagnet at 400 °C are shown in Fig. 3(a-d), respectively. Whereas the broad peak at ca. 3661-3482 cm^{-1} are due to OH stretching vibrations of adsorbed water, observation of two vibrations at 1600-1400 cm^{-1} region are attributed to COO^- groups (Fig. 3(a)). In Fig 3(b), while the vibration bands appearing at 2946 and 2869 cm^{-1} are due to the CH_2 groups of acetyl acetone (AcAc) and vibrations displaying at the regions 1709 and 1619 cm^{-1} are related to the C=O and C=C groups, respectively. The peaks observed around 1500 cm^{-1} are attributed to the rotational vibration of AcAc C-C-C, C-C-O and OH groups [17].

In Fig. 3(c), whereas the vibration of AcAc functional group are still seen in the as prepared hybrid material prior to calcination, but these peaks disappear after calcination at 400 °C and a new peak with low intensity

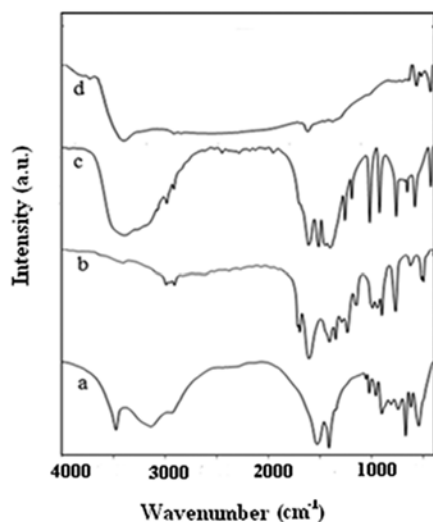


Fig. 3. FT-IR spectra of (a) nickel acetate tetrahydrate, (b) acetyl acetone, (c) as-prepared hybrid complex under reflux and (d) Ni/NiO MNPs.

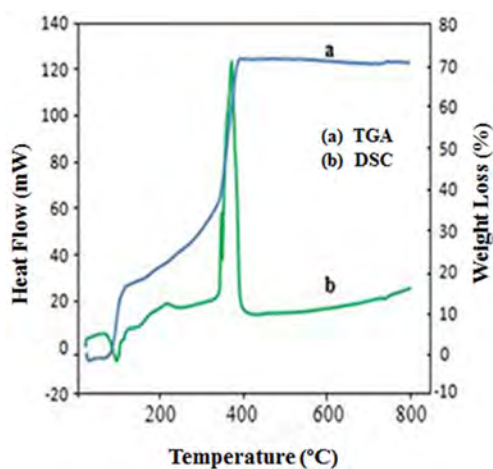


Fig. 4. TGA-DSC curves of NiO precursor; (a) TGA and (b) DSC.

is observed at 480 cm^{-1} due to the Ni-O vibration (Fig. 3(d)) [18].

To show the occurring changes during the thermal treatment of the precursor powders obtained in refluxing process, TGA and DSC analysis were carried out on the sample heated over 20 to 800 °C under atmosphere. As indicated in TG curve (Fig. 4), the major weight loss occurs below 400 °C. It also shows a weight loss of 20% in the temperature range of 80-100 °C due to the evaporation of the absorbed water. An exothermic peak at approximately 371 °C occurs in DSC, which might be associated with the conversion of precursor to Ni/NiO and also the decomposition of the organic residues. This process has the weight loss of about 52%. Weight losses hardly have occurred above 410 °C, indicating that the decomposition reaction was almost finished.

The magnetic property of Ni/NiO nanoparticles, magnetization versus magnetic field plot (M-H loop) is shown in Fig. 5. The saturation magnetization (M_s) for the prepared Ni/NiO nanoparticles is 28.44 emu g^{-1} ($1 \text{ emu g}^{-1} = 1 \text{ Am}^2 \text{ kg}^{-1}$) which is smaller than that of bulk nickel (55 emu/g) [33] perhaps due to the thin layer of NiO in which the presence of nickel oxide has been confirmed by XRD data. Tracy *et al.* [34]

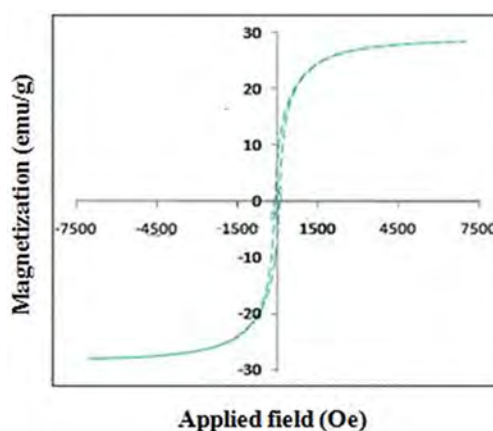


Fig. 5. Magnetization versus applied field for Ni/NiO MNPs.

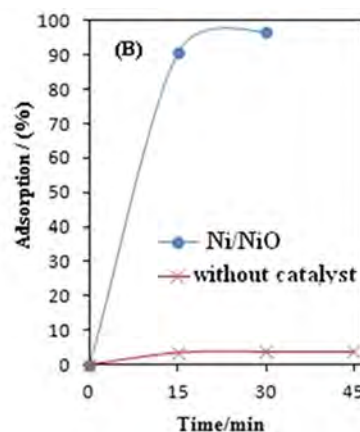
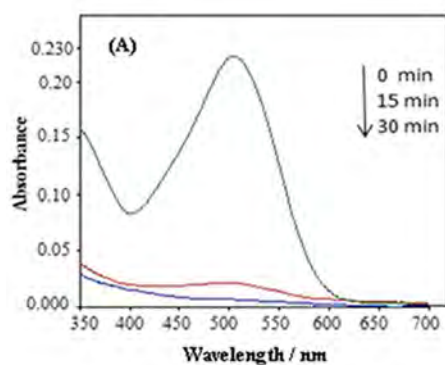


Fig. 6. Variation of the UV absorption spectra of Congo red solution in the presence of (A) Ni/NiO MNPs and (B) efficiency of adsorption as a function of time at 497 nm.

reported the growth of nickel oxide shells on nickel nanoparticles and confirmed the decrease in M_s values due to the NiO formation. The detailed M_s values depend on the Ni core size and shell thickness [35]. As shown in Fig. 5, the hysteresis behavior reveals that the nanocrystals are ferromagnetic and symmetric with respect to the zero magnetic fields. In nanometer-sized Ni/NiO, the overall magnetic behavior comprising magnetic nanocrystals of Ni and NiO, is a result of the properties of the individual constituents. However, these nanocrystal assemblies contain an interface between a ferromagnet (FM; Ni) and an antiferromagnet (AFM; NiO), exhibiting an additional unidirectional anisotropy owing to the magnetic coupling at the FM/AFM interface (exchange bias), which leads to magnetization stability in this case.

Monitoring of the dye adsorption was studied by determination of the decrease in the absorbance by a UV-Vis spectrophotometer (Fig. 6). Recall that the percentage of adsorption (X) shows the catalytic efficiency of the NiO as a function of time at 497 nm. Here $X = (C_0 - C) \times 100 / C_0$, where C_0 is the initial concentration of dye and C is the concentration of dye at time T . As indicated, the prepared Ni/NiO exhibits that 95% of Congo red has been eliminated after 30 min.

Conclusion

The Ni/NiO magnetic nanoparticles was synthesized using nickel salt, acetylacetonate as template and water as green solvent under reflux condition. The XRD results show the formation Ni/NiO with molar ratio 10/1. The TEM image approves the formation of nanoparticles with the average particle sizes 18-20 nm. Owing to magnetic coupling at the FM/AFM interface (exchange bias), the nanometer-sized Ni/NiO leads to the magnetization stability in this case. The experimental results demonstrated excellent magnetically separation of Congo-red by Ni/NiO (95%). Synthesis of stable magnetic nanoparticles in green solvent (water) via simple method over appropriate time and using cheap available chemicals are some advantages of this work. Further studies on functionalizing of the prepared nanoparticles and its catalytic behavior are currently under investigation in our laboratory.

Acknowledgments

The financial support from the University of Alzahra is gratefully acknowledged.

References

1. B.K. Nath, P.K. Chakrabarti, S. Das, U. Kumar, P.K. Mukhopadhyay, D. Das, *Eur. Phys. J. B* 39 (2004) 417-425.
2. C. Wang, X.M. Zhang, X.F. Qian, J. Xie, W.Z. Wang, Y.T. Qian, *Mater. Res. Bull.* 33 (1998) 1747-1751.
3. S. D'Addato, V. Grillo, S. Altieri, S. Frabbonia and S. Valeri, *Appl. Surf. Sci.* 260 (2012) 13-16.
4. V. Skumryev, S. Stoyanov, Y. Zhang, G. Hadjipanayis, D. Givord and J. Nogués, *Nature*. 423 (2003) 850.
5. J. Nogués, V. Skumryev, J. Sort, S. Stoyanov and D. Givord, *Phys. Rev. Lett.* 97 (2006) 157203-6.
6. R. Hao, R. Xing, Z. Xu, Y. Hou, S. Gao and S.H. Sun, *Adv. Mater.* 22 (2010) 2729-2742.
7. I. Brigger, C. Dubernet and P. Couvreur, *Adv. Drug. Deliv. Rev.* 54 (2002) 631-651.
8. A.K. Gupta and M. Gupt, *Biomaterials*. 26 (2005) 3995-4201.
9. A.H. Lu, E.L. Salabas and F. Schuth, *Angew. Chem. Int. Ed.* 46 (2007) 1222-44.
10. T.R. Sathe, A. Agrawal and S. Nie, *Anal. Chem.* 78 (2006) 5627-5632.
11. S. Laurent, D. Forge, M. Port, A. Roch, C. Robic, L.V. Elst and R.N. Muller, *Chem. Rev.* 108 (2008) 2064-2110.
12. W.Q. Jiang, H.C. Yang, S.Y. Yang, H.E. Horng, J.C. Hung, Y.C. Chen and C.Y. Hong, *J. Magn. Mater.* 283 (2004) 210-214.
13. G.M. de Costa, E. de Grave, P.M.A. de Bakker and R.E. Vandenberghe, *J. Solid State Chem.* 113 (1994) 405-412.
14. Y. Deng, L. Wang, W. Yang, S. Fu and A. Elaissari, *J. Magn. Mater.* 257 (2003) 69-78.
15. R. Abu Mukh-Qasem and A. Gedanken, *J. Colloid Interface Sci.* 284 (2005) 489-494.
16. D. Chen, R. Xu, *Mater. Res. Bull.* 33 (1998) 1015-1021.
17. T. Hyeon, S.S. Lee, J. Park, Y. Chung and H.B. Na, *J. Am. Chem. Soc.* 123 (2001) 12798-12801.
18. S. Basak, D.R. Chen, P. Biswas, *Chem. Eng. Sci.* 62 (2007) 1263-1268.
19. S. Veintemillas-Verdaguer, M.P. Morales and C.J. Serna, *Mater. Lett.* 35 (1998) 227-231.
20. W.H. Meiklejohn, C.P. Bean, *Phys. Rev.* 102 (1956) 1413-1414.
21. A.E. Berkowitz and K. Takano, *J. Magn. Mater.* 200 (1999) 552-570.
22. A. Roy, V. Srinivas, S. Ram, J.A. de Toro and J.M. Riveiro, *J. Appl. Phys.* 96 (2004) 6782-6788.
23. S.A. Makhlof, F.T. Parker, F.E. Spada and A.E. Berkowitz, *J. Appl. Phys.* 81 (1997) 5561-5563.
24. J.B. Tracy, D.N. Weiss, D.P. Dinega and M.G. Bawendi, *Phys. Rev. B* 72 (2005) 064404.
25. S. Cabanas-Polo, R. Bermejo, B. Ferrari and A.J. Sanchez-Herencia, *Corrosion Science*. 55 (2012) 172-179.
26. Y.H. Qi, P. Bruckel and P. Lours, *J. Mater. Sci. Lett.* 22 (2003) 371-374.
27. C. Liu, A.M. Huntz and J.L. Lebrun, *Mater. Sci. Eng. A* 160 (1993) 113-126.
28. A.M. Huntz, M. Andrieux and R. Molins, *Mater. Sci. Eng. A* 415 (2006) 21-32.
29. A.M. Huntz, M. Andrieux and R. Molins, *Mater. Sci. Eng. A* 417 (2006) 8-15.
30. C. Namasivayam and D. Kavitha, *Dyese & Pigments*. 54 (2002) 47-58.
31. V. Vimonses and S. Lei, B. Jin, C.W.K. Chow, C. Saint, *Chem. Eng. J* 148 (2009) 354.
32. F.A. Pavan, S.L.P. Dias, E. C. Lima and E.V. Benvenutti, *Dyese & Pigments*. 76 (2008) 64-69.
33. J.H. Hwang, V.P. Dravid, M.H. Teng, J.J. Host, B.R. Elliott, D.L. Johnson and T.O. Mason, *J. Mater. Res.* 12 (1997) 1076.
34. A.C. Johnston-Peck, J.W. Wang and J.B. Tracy, *ACS Nano*. 3 (2009) 1077.
35. H. Chen, C. Xu, C. Chen, G. Zhao and Y. Liu, *Mater. Res. Bull.* 47 (2012) 1839-1844.